Mechanism of nucleation and growth of cubic boron nitride thin films

D.V. Shtansky[a,*], Y. Yamada-Takamura[a], T. Yoshida[a], Y. Ikuhara[b]

[a]*Department of Materials Engineering, Graduate School and Faculty of Engineering, The University of Tokyo, 7-3-1 Hongo, Bunkyo-ku, Tokyo 113-8656, Japan*
[b]*Engineering Research Institute, School of Engineering, The University of Tokyo, 2-11-16 Yayoi, Bunkyo-ku, Tokyo 113-8656, Japan*

Abstract

The mechanism and the crystallography of the nucleation and growth of cubic boron nitride (c-BN) films deposited on $\langle 100 \rangle$-oriented silicon substrate by RF bias sputtering have been studied by means of cross-sectional high-resolution transmission electron microscopy and X-ray photoelectron spectroscopy. Both methods provide experimental information showing no sp^2-bonded BN layer formation in the subsurface region of c-BN phase. This is clear evidence for layer-by-layer homoepitaxial growth of cubic boron nitride without graphitic monolayers in the near-surface region of the film. The turbostratic boron nitride (t-BN) consists of thin sub-layers, 0.5–2 nm thick, growing in such a way that a sub-layer normal is almost parallel to the growth direction. t-BN also comprises a large volume fraction of the grain boundaries with high interface energies. The present result and the finding by Shtansky et al. [Acta Mater. 48, 3745 (2000)], who showed that an individual sub-layer consists of parallel lamellae in both the hexagonal (h-BN) and rhombohedral (r-BN) configurations, demonstrate that high intrinsic stress in the films is due to the complex structure of sp^2-bonded BN. The crystallography of c-BN films indicates heteroepitaxial nucleation of cubic phase on the graphitic BN structural precursor. The present results are consistent with stress-induced c-BN formation. © 2001 Published by Elsevier Science Ltd.

Keywords: Cubic boron nitride films; Turbostratic boron nitride; Growth models

1. Introduction

The mechanism of growth of cubic boron nitride (c-BN) films has been studied quite intensively because of the importance of c-BN in view of its outstanding chemical, thermal and mechanical properties. In an attempt to provide a quantitative description of the c-BN growth mechanism, six different growth models have been proposed (compressive stress model [1,2], dynamic stress (momentum transfer) model [3–6], preferential (selective) sputter model [7,8], subplantation model [9–12], cylindrical thermal spike model [13–15], and nanoarches model [16], neither of them account for all the experimental results available. There are several excellent review papers surveying current theories of c-BN nucleation and growth [16–18]. The c-BN growth occurs by a mechanism in which the structural changes are accomplished by several features such as high compressive stress of several GPa; growth of a layered structure consisting of an amorphous (a-BN) interface layer, followed by textured sp^2-bonded BN, and a final layer of c-BN; existence of a window of bias voltage values and sharp threshold values for ion energy. Recently, attempts have been made to revise some basic principles of c-BN growth on the basis of new experimental results. Cardinale et al. [19] argued that the observed textures of sp^2-bonded layer are not those that minimize elastic strain energy as was proposed by McKenzie et al. [1]. The results by Feldermann et al. [14] and Schwarz et al. [20] revealed that the growth of c-BN is less affected by substrate temperature than those accepted previously. McCarty et al. [21] also suggested that the thresholds for c-BN nucleation and growth are different as far as both the substrate temperature and ion energy are concerned, and the c-BN growth requires softer process parameters. Several works [22–24] indicated that the near-surface region of the growing c-BN film exhibits sp^2-bonded monolayers that were taken as indications of either the ion-induced compressive stress [22,24] or the subplantation [23] model. The importance of crystallography in the c-BN film growth leads to a remarkable rationalization of the observed interface planes and orientation relationships between the c-BN, hexagonal (h-BN) and rhombohedral (r-BN) constituents. Shtansky et al. [25] demonstrated

* Corresponding author. Present address: SHS-Center, Moscow Steel and Alloys Institute, Leninsky pr. 4, 164, Moscow 119991, Russia. Tel.: +7-095-236-5298; fax: +7-095-236-5298.
E-mail address: shtansky@shs.misis.ru (D.V. Shtansky).

that crystallography operates from the earliest stage of the c-BN film growth and specific orientation relationships were fulfilled between the h-BN and r-BN phases in the turbostratic BN (t-BN) layer and between the cubic phase and its structural precursors during the c-BN nucleation.

The purpose of this paper is to present some new observations of structural evolution of c-BN films, which allow the mechanism of c-BN nucleation and growth to be further discussed.

2. Experimental procedure

Cubic BN films were deposited on $\langle 100 \rangle$-oriented silicon wafers by RF bias sputtering in argon using a sintered hexagonal BN target (KD-3S, ShinEtsu Kagaku). The total gas pressure was maintained at 16 mTorr. The target input RF power was 600 W and the applied substrate bias voltage was kept to -300 V. Prior to deposition, the target was presputtered for 15 min, the shutters between the electrodes being close. The deposition time ranged from 3 to 5 min that resulted in the film thickness of about 40–100 nm.

In order to examine the bonding state of the film surface, angle resolved X-ray photoelectron spectroscopy (XPS) was carried out. An X-ray photoelectron spectrometer (XPS-7000, Rigaku Denki) with an X-ray source of non-monochromatized MgKα radiation (1253.6 eV) was used. The hemispherical analyzer was operated at 25 eV path energy. The electron take-off angle (θ) relative to the sample surface normal was gradually changed from 0 to 70°. The depth d, which produces majority of the total signal, equals inelastic mean free path (λ) when $\theta = 0$, whereas the depth $d = \lambda \cos \theta$ becomes smaller as θ is increased.

Thin foils for cross-sectional high-resolution TEM studies were prepared using a standard technique involving sticking of two film/substrate pieces together by epoxy with the films facing each other, cutting slices normal to the interface plane, and then mechanical grinding and dimpling. The specimens were attached by epoxy to stainless steel rings for reinforcement. Subsequently, they were subjected to ion-milling to perforation at a voltage of 4 kV and finally using a cold stage (liquid N_2) at 2.5 kV in order to minimize damage to the specimen. The structure of the films was examined in a Hitachi-9000NAR transmission electron microscope with the point resolution of 0.19 nm operating at 300 kV.

3. Experimental results

3.1. Imperfections in sp²-bonded layer

It is usually believed that intensive ion irradiation creates a high density of point defects in the near-surface region of the films. The accumulation of defects and the atomic rearrangement in the topmost surface layer of a few nanometers results in high levels of ion-induced residual compressive stress and local dynamic strain which are considered to promote the formation of cubic phase [2,4]. It has been shown that the compressive stress in sp²-bonded BN layer increased gradually with increasing film thickness [26,27]. Fig. 1 shows a cross-sectional HRTEM image of a typical area of sp²-bonded BN. This area exhibited the well-developed parallel fringes with the d spacing consistent with the value of about 0.33 nm, which is characteristic of basal planes of the h-BN and r-BN phases those are oriented edge on. The image revealed a number of layer boundaries as shown by arrows. It can be seen that the sp²-bonded BN grew in a layered fashion in such a way that a sub-layer normal made relatively small angle with the film-growth direction. The thickness of individual sub-layer was estimated to be approximately 0.45–2 nm. This is extremely small thickness, being only a few unit cells in dimension. Across the interfaces, atomic basal planes were not perfectly matched, since extra half planes were frequently visible on either side of the interface. Recently, it has been demonstrated [25] that each sp²-bonded sub-layer consists of parallel lamellae in both the h-BN and r-BN configurations. Thus, rather than the concentration of point defects [4], the structural features described above appeared to produce high volumetric stress in the turbostratic layer of the c-BN
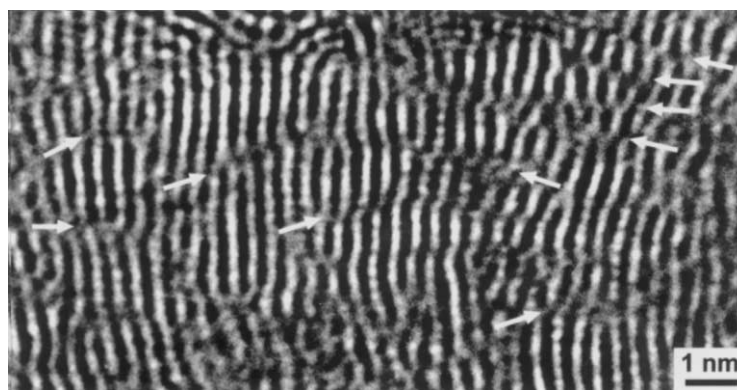

Fig. 1. Cross-sectional HRTEM image showing that the sp²-bonded BN region consists of thin sub-layers, 0.5–2 nm thick, with a sub-layer normal almost parallel to the film growth direction. Arrows indicate the positions of layer boundaries.

films. Moreover, if we assume the origin of intrinsic film stress by a high concentration of point defects, one would expect that c-BN nucleation show temperature dependence, since high temperature deposition should lead to defect relaxation, but such a trend is not observed experimentally. In contrast, intrinsic compressive stress due to the small grain size and large volume fraction of grain boundaries with high strain energies appear to be rather insensitive to substrate temperature.

3.2. Near-surface structure of sp³-bonded layer

The near-surface region of the c-BN films has been reported to comprise several sp^2-bonded BN monolayers [22–24], providing further credence for the subplantation model. This result has been taken as an indication that the transformation to c-BN occurs at the sub-surface region of the growing film [4], whereas the mechanism of sp^2 surface reconstruction, predicted by the sputter model [7], is brought in question [23]. Fig. 2(a) and (b) show B 1s XPS spectra for the c-BN film and sp^2-bonded pyrolitic BN,
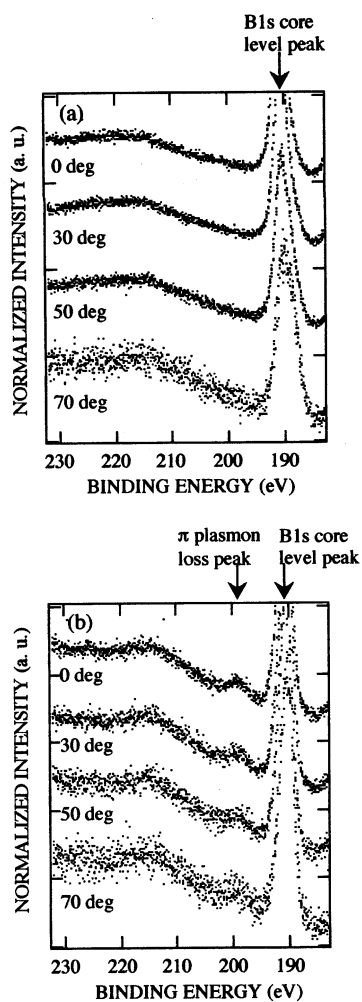
respectively. The spectra were normalized by setting the core level peaks to unity. The sp^2-bonded BN exhibited one distinct major peak, positioned at about 190 eV, and a π plasmon loss feature at about 9 eV higher binding energy than the core level peak. In contrast, no evidence for the existence of h-BN was observed for c-BN film spectra. In order to evaluate inelastic mean free path (λ) of photoelectron with an energy of 1000 eV, Tanuma, Powell and Penn's [28] formula using bulk properties of c-BN (density 3.5 g/cm³, band gap 6–8 eV) and h-BN (density 2.3 g/cm³, band gap 3–6 eV) was applied and the values of about 2.1–2.2 and 1.9–2.0 nm were obtained, respectively. The density and the band gap energy of the deposited films are considered to be different from those of the bulk materials, but even if the density of sp^2-bonded BN phase was as low as 1.5 g/cm³, λ and d at $\theta = 70°$ are equal to 1.9–2.0 and 0.65–0.70 nm, respectively. This result indicates that even if the superficial layer of sp^2-bonded BN existed on the growing surface of the c-BN layer, its thickness should be considerably smaller in comparison with the actual escape depth of photoelectrons of 0.7 nm.

High-resolution transmission electron microscopy (HRTEM) is another powerful tool to reveal the atomic structure of near-surface region of the c-BN film. Fig. 3 shows a c-BN crystallite with a lateral grain size of 20 nm located 40 nm away from the film/substrate interface and oriented along a ⟨110⟩ zone axis. Therefore, both sets of {111} planes are visible as indicated in the HRTEM micrograph. The HRTEM characterization confirmed that the top layer of the film, 20 nm thick, consisted of almost pure cubic phase. The surface of the film adjoined the area of epoxy displaying an image of randomly scattered intensities at the atomic scale, which is characteristic of an amorphous structure. The interface between the c-BN film and epoxy was observed almost at the edge-on condition, since the thickness fringes due to the boundaries were not visible. Thus, in agreement with the XPS results, the presence of a topmost layer of sp^2-bonded graphitic BN can hardly be recognized. This is clear evidence for layer-by-layer homoepitaxial growth of cubic phase without intermediate layer. Note
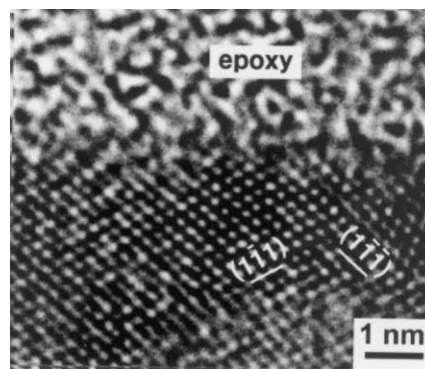

Fig. 2. B 1s XPS spectra from: (a) c-BN film; and (b) sp^2-bonded pyrolitic BN.

Fig. 3. Cross-sectional HRTEM image of a single c-BN crystallite showing that there is no sp^2-bonded BN monolayers in the near-surface region of the film. The incident beam direction is $[110]_{c\text{-BN}}$.

that this result does not imply that once c-BN is nucleated, it continues to grow without further transformation. Shtansky et al. [25] showed that a thin layer, 1–2 nm, of sp^2-bonded BN could form between the c-BN grains to reduce the grain boundary energy.

3.3. Crystallography of c-BN nucleation

It has been shown that the c-BN phase nucleates on the oriented graphitic BN layer in a semicoherent manner and obeys specific orientation relationships with the hexagonal and rhombohedral phases [25]. Thus, part of the total driving free energy for nucleation must be spent on the creation of a new interface between the c-BN crystallite and its structural precursor. It is also evident that the nucleation of c-BN is easy to achieve if a specific orientation relationship can be fulfilled. Fig. 4 is a cross-sectional HRTEM micrograph showing the layered structure of the c-BN film where the atomic structure of each layer could be recognized. It can be seen that the c-BN film consisted of an
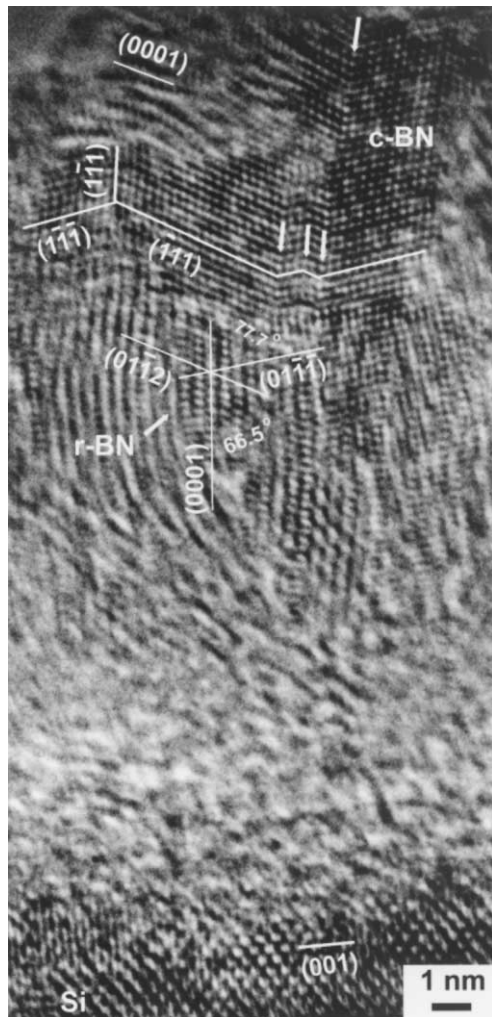

Fig. 4. Cross-sectional HRTEM image showing the layered structure of c-BN film, where the crystallography of the sp$^2 \rightarrow$ sp^3 transformation can be seen. The incident beam direction is $[110]_{Si}//\langle110\rangle_{c-BN}//[2\bar{1}\bar{1}0]_{r-BN}$.

amorphous layer, 6 nm, at the film/substrate interface, followed by preferentially oriented sp^2-bonded BN, 6 nm, and a final layer of c-BN. The specimen was sufficiently well aligned with the $[110]_{Si}//\langle110\rangle_{c-BN}//[2\bar{1}\bar{1}0]_{r-BN}$ direction. The observed periodicities within the basal planes and the angles between sets of fringes in sp^2-bonded region were consistent with those for the r-BN structure. The basal planes of r-BN formed parallel with the c-BN twin planes in agreement with previous results [25]. Thus, the following orientation relationships between the c-BN and r-BN were fulfilled:

$$[2\bar{1}\bar{1}0]_{r-BN}//[\bar{1}\bar{1}0]_{c-BN} \qquad [2\bar{1}\bar{1}0]_{r-BN}//[110]_{c-BN}$$

$$(01\bar{1}\bar{1})_{r-BN}//(1\bar{1}\bar{1})_{c-BN} \qquad (01\bar{1}2)_{r-BN}//(\bar{1}11)_{c-BN}$$

$$(0001)_{r-BN}//(1\bar{1}1)_{c-BN} \qquad (0001)_{r-BN}//(1\bar{1}1)_{c-BN}$$

It can also be seen that the c-BN crystallite transformed to the sp^2-bonded BN during subsequent growth in such a way that the $\{111\}_{c-BN}$ close packed planes were parallel to the basal planes of graphitic BN. Some would suggest that this was just a part of the sp^2-bonded BN growing beside the c-BN crystallite, but the different orientation of the basal planes indicated that these were different t-BN crystallites. Note that the atomic matching between the $\{111\}_{c-BN}$ planes of c-BN and the basal planes of t-BN consisted of both the plane-on-plane and edge-on-edge matching. This result demonstrates that during the growth of boron nitride films, c-BN and t-BN crystallites maintained good atomic matching, resulting in minimization of strain energy at the interfaces.

4. Discussion

The results presented here are qualitatively consistent with the model of stress-induced c-BN formation. The various types of stress during the growth of the c-BN film are shown in Fig. 5. The main criteria, which may play a key role for the nucleation of c-BN, are summarized below.

1. High compressive stress of several GPa seems to be necessary for the deposition of c-BN films [26,27,29,30]. Some recent results are also consistent with the model of stress-induced c-BN formation, such as the highest c-BN percentage in films grown on hard substrates [31], nucleation of cubic phase on β-SiC/Si substrate without intermediate sp^2-bonded BN layer [32], and consecutive growth of c-BN on a previously nucleated c-BN film [14].

2. The complex structure of the sp^2-bonded BN is highly strained. The t-BN consists of thin sub-layers, 0.5–2 nm thick, consisting of parallel lamellae in both the h-BN and r-BN configurations. It also comprises a large volume fraction of the grain boundaries with high interface energies. All these observations agree well with the results by Fitz et al. [27] that the stress in t-BN layer increases with the film
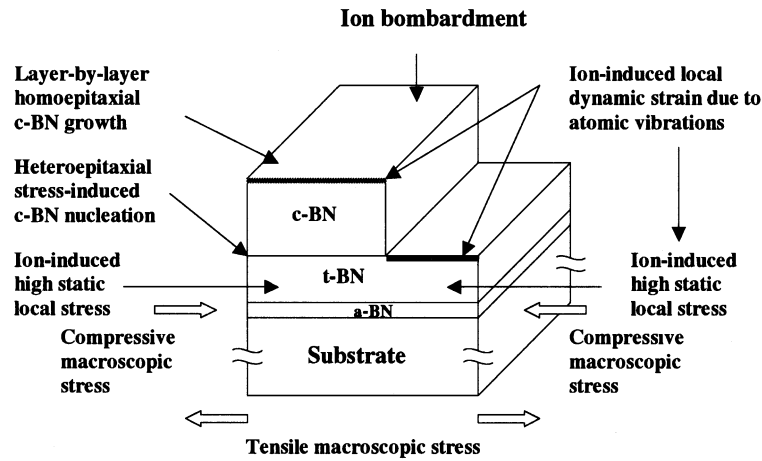
Fig. 5. Growth of c-BN film (schematic) with the various types of stress indicated.

thickness. In view of these arguments the existence of a critical thickness of the intermediate layer required for c-BN nucleation, which also depends significantly upon the bombarding ion energy, can easily be understood. Several models assume that the volumetric strains due to atomic displacements result in the film stress. It is not clear whether relaxation or accumulation of structural defects takes place behind the growing film surface. In all these cases, however, atomic displacements were calculated from theory and not experimental determinations, and therefore may be questionable. Although HRTEM is not a perfect method to reveal point defects, only twinning about the close-packed planes in c-BN crystallites was observed, as far as imperfections are concerned. As was pointed out by Collazo-Davila [16] the major shortfall of the compressive stress model is their inability to explain the effect of the substrate temperature since higher temperatures should allow for more defect relaxation process to occur, thus decreasing the dynamic stress. In contrast, from the present results, one may conclude that a high compressive stress in the film is due to the complex structure of the sp^2-bonded BN, which is not affected by temperature to a great extent, although the contribution of ion-induced atomic rearrangement cannot completely be excluded. It should be noted that the internal stress in the films have been measured both in situ [27,30] and after deposition by bending method [26,29] or using the sin$^2 \psi$ method of XRD [33] and the results obtained agree fairly well. Thus, the structure of t-BN observed here is expected to reflect the intrinsic strained state of the film.

3. No evidence for the existence of sp^2-bonded BN in the near-surface region of cubic layer was seen under the deposition conditions used in the present study. This result suggests that layer-by-layer homoepitaxial growth of c-BN occurred. Thus, both the subplantation and dynamic stress models, predicting the formation of c-BN at a depth corre-

sponding the high concentration of point defects, come into question. Note that the sp^2-bonded BN observed in the near-surface region by either XPS [22,24] or REELS [23] analysis can be attributed to the existence of graphitic layers formed between the c-BN grains [25,34].

4. It is worth to mention that the growth of c-BN films proceeds under similar ion-bombardment conditions during one series, all process parameters being kept constant. Thus, the question arises as to why does a thick intermediate sp^2-bonded BN layer, 40–50 nm, develops frequently before the cubic phase starts to grow. This result cannot be explained only by a dynamic atomic-scale lattice strain in the near-surface region of the film caused by ion bombardment. It seems reasonable to conclude that various kinds of stress, such as high macroscopic, microscopic dynamic and static film stress are essential factors for the nucleation of c-BN from t-BN. In view of similar arguments, the quenching of thermal spikes caused by atomic rearrangement in the ion impact near-surface region, cannot account for the formation of cubic phase.

5. It is well known that the stress is a function of ion energy and ion-to-atom arrival ratio, which can be described in terms of the momentum transferred to the film by ions [4,35]. The present results support this conclusion. It was observed that the concentration of imperfections in t-BN layer, such as high-energy grain boundaries, twin boundaries and extra half planes, decreased under less intensive ion bombardment.

6. It has been shown that c-BN films can be grown at low deposition temperatures down to 120°C [20] or even at room temperature [14]. In the last case the c-BN film was deposited on the c-BN layer previously nucleated on Si substrate. Thus the substrate temperature is not a key factor controlling the growth of cubic phase.

7. The present and previous [25] results reveal the great role of crystallography during the development of c-BN films. The c-BN phase nucleates on the oriented graphitic

BN layer in a semicoherent manner and obeys specific orientation relationships. Thus the oriented t-BN acts as a structural precursor for c-BN formation. The critical free energy for nucleation is a consequence of the free energy/ area of the interface between the nucleus and precursor phase. It is well known that the specific orientation relationship yields low interface energy. Thus the formation of intermediate sp^2-bonded BN layer provides the favorable boundary conditions for c-BN nucleation. The growth of highly twinned c-BN crystallites with twinning occurring about a single type of {111} planes is understood in terms of good atomic matching between the {111} close-packed plane of c-BN parallel to either the $(01\bar{1}2)_{r-BN}$ or $(01\bar{1}\bar{1})_{r-BN}$ plane of r-BN most parallel to the grain boundary, yielding a low interface energy. Further away from the sp^2-bonded BN layer, twinning about more than one of the sets of $\{111\}_{c-BN}$ planes has been observed [25]. These crystallographic features for the c-BN nucleation and growth are consistent with the stress-induced solid-state $sp^2 \rightarrow sp^3$ transformation.

8. Some of the supporters of the stress model suppose that the high pressure from the local instantaneous and residual compressive stress pushes the system into a region of the phase diagram where the cubic phase is stable. Recent results [36], however, showed that cubic boron nitride is a thermodynamically stable modification at atmospheric pressure and temperatures up to 1600 K. Note that there are still disagreements concerning whether the phase composition of the films deposited under non-equilibrium conditions can be predicted from the equilibrium phase diagram as was proposed by Gissler and co-workers [37,38] in Ti–B–N system but was not confirmed by Shtansky et al. [39], who reported that the equilibrium phase diagram fails to predict correctly the phase composition of the Ti–Al–B–N films. In any case, the metastable phase may nucleate in favor of a stable one. Such kinetic barriers to precipitation of equilibrium phase are well known [40].

5. Conclusions

1. HRTEM and XPS provided clear experimental evidence for layer-by-layer homoepitaxial growth of c-BN thin films without formation of sp^2-bonded BN monolayers in the sub-surface region of the film.
2. It was suggested that high intrinsic stress in the sp^2-bonded BN was due to its complex structure, comprising thin sub-layers, 0.5–2 nm thick, consisting of parallel lamellae in both the h-BN and r-BN configurations, and a large volume fraction of the grain boundaries with high interface energies.
3. Great role of crystallography in the c-BN nucleation mechanism was demonstrated. The formation of an initial sp^2-bonded BN layer provided the favorable boundary conditions for the heteroepitaxial nucleation of cubic phase.
4. The data obtained were compared with those reported

previously, and were discussed in terms of a mechanism operating the c-BN nucleation. The stress-induced c-BN formation has received further credence.

Acknowledgements

References

[1] D.R. McKenzie, D.J.H. Cockayne, D.A. Muller, M. Murakawa, S. Miyake, S. Watanabe, P. Fallon, Electron optical characterization of cubic boron nitride thin films prepared by reactive ion plating, J. Appl. Phys. 70 (1991) 3007–3012.

[2] D.R. McKenzie, W.D. McFall, W.G. Sainty, C.A. Davis, R.E. Collins, Compressive stress induced formation of cubic boron nitride, Diamond Relat. Mater. 2 (1993) 970–976.

[3] D.J. Kester, R. Messier, Phase control of cubic boron nitride thin films, J. Appl. Phys. 72 (1992) 504–513.

[4] P.B. Mirkarimi, K.F. McCarty, D.L. Medlin, W.G. Wolfer, T.A. Friedmann, E.J. Klaus, G.F. Cardinale, D.G. Howitt, On the role of ions in the formation of cubic boron nitride films by ion-assisted deposition, J. Mater. Res. 9 (1994) 2925–2938.

[5] D.L. Medlin, T.A. Friedmann, P.B. Mirkarimi, M.J. Mills, K.F. McCarty, Evidence for rhombohedral boron nitride in cubic boron nitride films grown by ion-assisted deposition, Phys. Rev. B 50 (1994) 7884–7887.

[6] D.L. Medlin, T.A. Friedmann, P.B. Mirkarimi, P. Rez, M.J. Mills, K.F. McCarty, Microstructure of cubic boron nitride thin films grown by ion-assisted pulsed laser deposition, J. Appl. Phys. 76 (1994) 295–303.

[7] S. Reinke, M. Kuhr, W. Kulisch, R. Kassing, Recent results in cubic boron nitride deposition in light of the sputter model, Diamond Relat. Mater. 4 (1995) 272–283.

[8] W. Kulisch, S. Reinke, Modeling of c-BN thin film deposition, Diamond Films Technol. 7 (1997) 105–138.

[9] Y. Lifshitz, S.R. Kasi, J.W. Rabalais, W. Eckstein, Subplantation model for film growth from hyperthermal species, Phys. Rev. B 41 (1990) 10 468–10 480.

[10] W. Dworschak, K. Jung, H. Ehrhardt, Growth mechanism of cubic boron nitride in a r.f. glow discharge, Thin Solid Films 254 (1995) 65–74.

[11] J. Robertson, J. Gerber, S. Sattel, M. Weiler, K. Jung, H. Ehrhardt, Mechanism of bias-enhanced nucleation of diamond on Si, Appl. Phys. Lett. 66 (1995) 3287–3289.

[12] S. Uhlmann, T. Frauenheim, U. Stephan, Molecular-dynamics subplantation studies of carbon beneath the diamond (111) surface, Phys. Rev. B 51 (1995) 4541–4546.

[13] H. Hofsäss, H. Feldermann, R. Merk, M. Sebastian, C. Ronning, Cylindrical spike model for the formation of diamondlike thin films by ion deposition, Appl. Phys. A 66 (1998) 153–181.

[14] H. Feldermann, R. Merk, H. Hofsäss, C. Ronning, T. Zheleva, Room temperature growth of cubic boron nitride, Appl. Phys. Lett. 74 (1999) 1552–1554.

[15] E. Franke, M. Schubert, J.A. Woollam, J.-D. Hecht, G. Wagner, H. Neumann, F. Bigl, In situ ellipsometry growth characterization of dual ion beam deposited boron nitride thin films, J. Appl. Phys. 87 (2000) 2593–2599.

[16] C. Collazo-Davila, E. Bengu, L.D. Marks, M. Kirk, Nucleation of

cubic boron nitride thin films, Diamond Relat. Mater. 8 (1999) 1091–1100.

[17] P.B. Mirkarimi, K.F. McCarty, D.L. Medlin, Review of advances in cubic boron nitride film synthesis, Mater. Sci. Engng R 21 (1997) 47–100.

[18] T. Yoshida, Vapour phase deposition of cubic boron nitride, Diamond Relat. Mater. 5 (1996) 501–507.

[19] G.F. Cardinale, D.L. Medlin, P.B. Mirkarimi, K.F. McCarty, D.G. Howitt, Orientation-dependence of elastic strain energy in hexagonal and cubic boron nitride layers in energetically deposited BN films, J. Vac. Sci. Technol. A 15 (1997) 196–200.

[20] G. Schwarz, F. Friess, G.K. Wolf, Deposition of c-BN by ion beam assisted CVD, Surf. Coat. Technol. 125 (2000) 106–110.

[21] K.F. McCarty, P.B. Mirkarimi, D.L. Medlin, T.A. Friedmann, J.C. Barbour, On the low-temperature threshold for cubic boron nitride formation in energetic film deposition, Diamond Relat. Mater. 5 (1996) 1519–1526.

[22] K.S. Park, D.Y. Lee, K.J. Kim, D.W. Moon, Growth mechanism of cubic boron nitride thin films by ion beam assist sputter deposition, J. Vac. Sci. Technol. A 15 (1997) 1041–1047.

[23] S. Ilias, V. Stambouli, D. Bouchier, Evidence for the layered structure of c-BN films by in situ REELS analyses and depth profiling, Appl. Surf. Sci. 152 (1999) 70–76.

[24] P. Widmayer, H.-G. Boyen, P. Ziemann, P. Reinke, P. Oelhafen, Electron spectroscopy on boron nitride thin films: comparison of near-surface to bulk electronic properties, Phys. Rev. B 59 (1999) 5233–5241.

[25] D.V. Shtansky, O. Tsuda, Y. Ikuhara, T. Yoshida, Crystallography and structural evolution of cubic boron nitride films during bias sputter deposition, Acta Mater. 48 (2000) 3745–3759.

[26] A. Klett, R. Freudenstein, M.F. Plass, W. Kulisch, Stress of c-BN thin films: a parameter investigation, Surf. Coat. Technol. 116/119 (1999) 86–92.

[27] C. Fitz, W. Fukarek, A. Kolitsch, W. Möller, Investigation on stress evolution in boron nitride films, Surf. Coat. Technol. 128/129 (2000) 292–297.

[28] S. Tanuma, C.J. Powell, D.R. Penn, Calculations of electron inelastic mean free paths (IMFPs) IV. Evaluation of calculated IMFPs and of the predictive IMFP formula TPP-2 for electron energies between 50 and 2000 eV, Surf. Interf. Anal. 20 (77) (1993) 77–89.

[29] G. Reisse, S. Weissmantel, Characterization of pulsed laser deposited h-BN films and h-BN/c-BN layer systems, Thin Solid Films 355/356 (1999) 105–111.

[30] M. Zeitler, S. Sienz, B. Rauschenbach, Study of stress evolution of boron nitride films prepared by ion assisted deposition, J. Vac. Sci. Technol. A 17 (1999) 597–602.

[31] P.B. Mirkarimi, K.F. McCarty, G.F. Cardinale, D.L. Medlin, D.K. Ottesen, H.A. Johnsen, Substrate effects in cubic boron nitride film formation, J. Vac. Sci. Technol. A 14 (1996) 251–255.

[32] P.B. Mirkarimi, D.L. Medlin, K.F. McCarty, J.C. Barbour, Growth of cubic BN films on β-SiC by ion-assisted pulsed laser deposition, Appl. Phys. Lett. 66 (1995) 2813–2815.

[33] X. Zhang, J. Yue, G. Chen, H. Yan, Study on stress and strain of cubic boron nitride thin films, Thin Solid Films 315 (1998) 202–206.

[34] W.-L. Zhou, Y. Ikuhara, M. Murakawa, S. Watanabe, T. Suzuki, Direct observation of hexagonal boron nitride at the grain boundary of cubic boron nitride by high resolution electron microscopy, Appl. Phys. Lett. 66 (1995) 2490–2492.

[35] T. Klotzbücher, E.W. Kreutz, Extended model for stress-induced formation of c-BN in ion-assisted deposition, Diamond Relat. Mater. 7 (1998) 1219–1226.

[36] V.L. Solozhenko, Current trends in the phase diagram of boron nitride, J. Hard Mater. 6 (1995) 51–65.

[37] W. Gissler, Structure and properties of Ti–B–N coatings, Surf. Coat. Technol. 68/69 (1994) 556–563.

[38] T.P. Mollart, M. Baker, J. Haupt, A. Steiner, P. Hammer, W. Gissler, Nanostructured titanium boron nitride coatings of very high hardness, Surf. Coat. Technol. 74/75 (1995) 491–496.

[39] D.V. Shtansky, K. Kaneko, Y. Ikuhara, E.A. Levashov. Characterization of nanocrystalline multiphase Ti–Al–B–N thin films with extremely small grain size. Submitted for publication.

[40] M. Hillert, in: H.I. Aaronson (Ed.), Lectures on the Theory of Phase Transformations, Metallurgical Society of AIME, Warrendale, Pennsylvania, 1975, p. 1.